iScience

CellPress
OPEN ACCESS

Article

SLC38A9 regulates SARS-CoV-2 viral entry

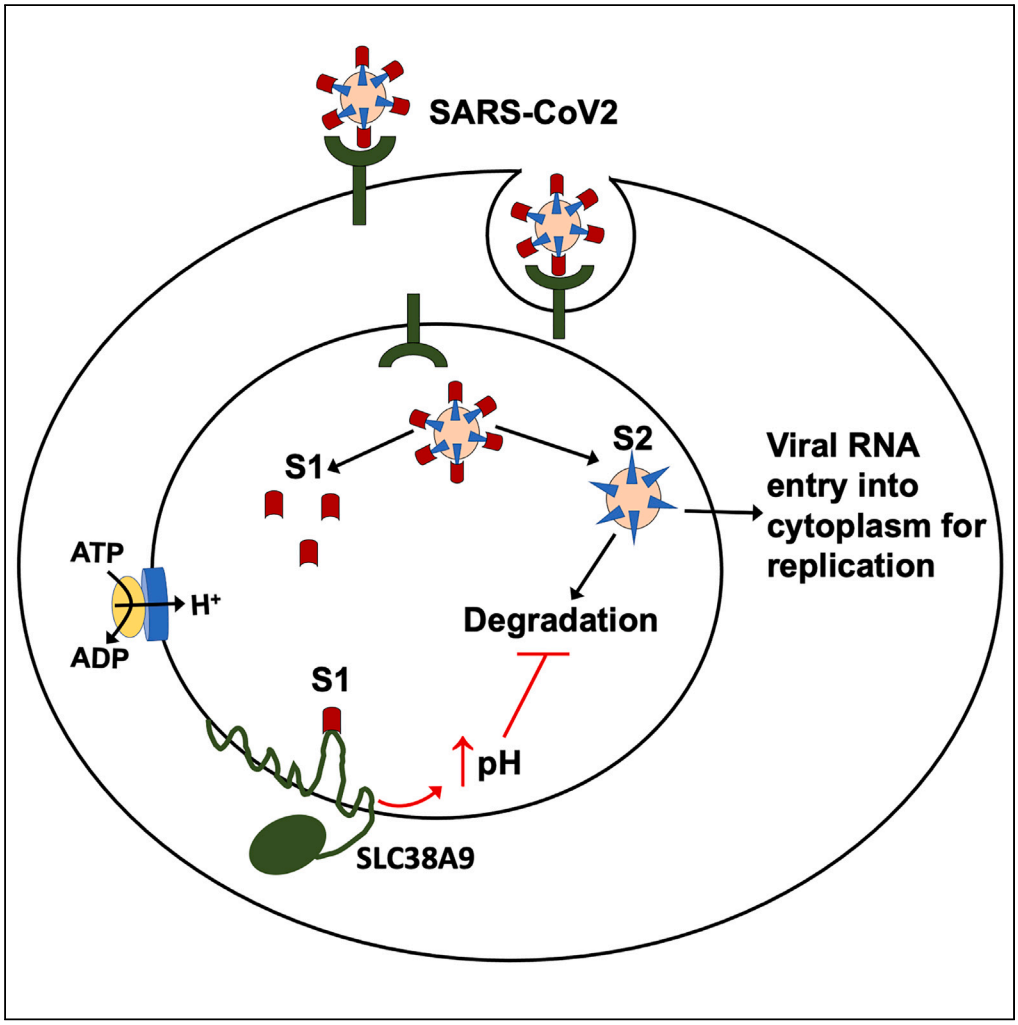

Gaurav Datta, Neda Rezagholizadeh, Wendie A. Hasler, Nabab Khan, Xuesong Chen

xuesong.chen@und.edu

Highlights

Multibasic motif of SARS-CoV-2 S1 is critical for its interaction with SLC38A9

SLC38A9 knockdown prevents SARS-CoV-2 S1-induced endolysosome de-acidification

SLC38A9 knockdown blocks S protein-mediated entry of pseudo-SARS-CoV-2

Datta et al., iScience 27, 110387
July 19, 2024
https://doi.org/10.1016/j.isci.2024.110387

iScience

CellPress
OPEN ACCESS

Article

SLC38A9 regulates SARS-CoV-2 viral entry

Gaurav Datta,[1] Neda Rezagholizadeh,[1] Wendie A. Hasler,[1] Nabab Khan,[1] and Xuesong Chen[1,2,*]

SUMMARY

SARS-CoV-2 viral entry into host cells depends on the cleavage of spike (S) protein into S1 and S2 proteins. Such proteolytic cleavage by furin results in the exposure of a multibasic motif on S1, which is critical for SARS-CoV-2 viral infection and transmission; however, how such a multibasic motif contributes to the infection of SARS-CoV-2 remains elusive. Here, we demonstrate that the multibasic motif on S1 is critical for its interaction with SLC38A9, an endolysosome-resident arginine sensor. SLC38A9 knockdown prevents S1-induced endolysosome de-acidification and blocks the S protein-mediated entry of pseudo-SARS-CoV-2 in Calu-3, U87MG, Caco-2, and A549 cells. Our findings provide a novel mechanism in regulating SARS-CoV-2 viral entry; S1 present in endolysosome lumen could interact with SLC38A9, which mediates S1-induced endolysosome de-acidification and dysfunction, facilitating the escape of SARS-CoV-2 from endolysosomes and enhancing viral entry.

INTRODUCTION

Infection by severe acute respiratory syndrome-coronavirus-2 (SARS-CoV-2) causes the current pandemic of coronavirus disease 2019 (COVID-19),[1,2] which has resulted in over 771 million confirmed cases and 6.9 million deaths (https://www.who.int/emergencies/diseases/novel-coronavirus-2019). Persistence of SARS-CoV-2 virus[3–6] and/or viral proteins[7–9] also contributes to the development of long COVID,[10] which affects 6% of US adults.[11]

SARS-CoV-2 is an enveloped single-stranded RNA virus, and like other enveloped viruses, SARS-CoV-2 enters host cells where it utilizes host cell machinery for replication. The spike protein (S protein) on the outer surface of SARS-CoV-2 is responsible for its cell attachment and internalization[12,13] via cell surface receptors including ACE2,[14] neuropilin-1[15,16], and others.[17] The entry of SARS-CoV-2 into host cells depends on the cleavage of S protein into S1 and S2 proteins at S1/S2 site and subsequent S2′ site[18,19] by various cellular proteases of the host including transmembrane protease serine 2 (TMPRSS2),[20–23] furin,[24,25] and cathepsin L.[21] Once cleaved, a hydrophobic fusion peptide, located immediately downstream of the S2′ cleavage site in the S2 subunit, will be exposed, which mediates the fusion of viral membrane with host cell membrane.[26,27] S2 could mediate the fusion of the viral envelope with plasma membrane of host cells at the cell surface or with endosome membrane following its endocytosis.[12,25,28,29] Once fused with host cell membrane, viral RNA is released into the cytosol, where viral replication occurs.[30,31]

The cleavage of S proteins by furin results in the exposure of a multibasic motif with multiple arginine (RRAR) on the C-terminus of S1, located at the S1/S2 junction.[24,25] The presence of such an multibasic motif distinguishes SARS-CoV-2 from SARS-CoV-1 that caused SARS outbreak in 2002–2003 and all other known sarbecoviruses whose S protein is not cleaved by furin proteases.[23–25,28] Importantly, the cleavage at the S1/S2 site by furin destabilizes S protein and promotes its binding to ACE2 and subsequent cleavage at the S2′ site, which is critical for S2-mediated fusion and viral infection.[18,19,24,32] The lack of the multibasic motif impairs SARS-CoV-2 viral entry into the host cells.[15] One explanation for why the multibasic motif of S1 enhances viral entry is that the multibasic motif of S1 could bind neuropilin-1 to promote S1 shedding, the exposure of the S2′ site to TMPRSS2,[33] and subsequent viral fusion at the plasma membrane.[34]

However, SARS-CoV-2 infects multiple organs and systems.[35] If the target cells express insufficient TMPRSS2 or if a SARS-CoV-2 does not encounter TMPRSS2,[32,34,36] SARS-CoV-2 could enter host cells via receptor-mediated endocytosis with the assistance of ACE2[12] or integrin[37] into endosomes. Furthermore, multiple routes of antibody-opsonized SARS-CoV-2 infection of host cells[38–41] could lead to the entering of SARS-CoV-2 into endosomes via antibody-mediated endocytosis. In the lumen of endosomes, S protein can also be cleaved into S1 and S2 by cathepsin L,[42,43] and S2 could mediate fusion of viral membrane with endosome membrane and endosome-dependent viral entry into host cells. Furthermore, the S1/S2 site of the S protein can be cleaved by furin during virus particle formation.[19] The cleaved S1 could interact with S2 as heterodimer possibly via a non-covalent interaction, and factors that interrupt such an interaction could lead to the dissociation of S1 from S2; For example, the binding of S1 to neuropilin-1 could promote the separation of S1 from S2.[33] Dissociation of S1 proteins from the viral membrane results in their release into the bodily fluids,[7,44] and such dissociated S1 can also enter host cell endosomes via receptor-mediated endocytosis.[12,45,46]

[1]Department of Biomedical Sciences, University of North Dakota School of Medicine and Health Sciences, Grand Forks, ND 58203, USA
[2]Lead contact
*Correspondence: xuesong.chen@und.edu
https://doi.org/10.1016/j.isci.2024.110387

Given that endolysosomes, referring to the endosomal-lysosomal system, are critical for the degradation of internalized SARS-CoV-2 virus and viral proteins,[12] here we addressed question of whether the multibasic motif (RRAR) of S1 could interact with an endolysosome-resident protein and regulate viral entry. We demonstrated that the multibasic motif of S1 is critical for its interaction with SLC38A9, an endolysosome-resident arginine sensor.[47–49] SLC38A9 knockdown prevents S1-induced endolysosome de-acidification and blocks the S protein-mediated entry of pseudo-SARS-CoV-2.

RESULTS

The multibasic motif of SARS-CoV-2 S1, which is critical for its endolysosome de-acidifying effect, interacts with SLC39A9

SARS-CoV-2 virus could enter host cells via receptor-mediated endocytosis[12,37] into endosomes, where S1 can be generated following the proteolytic cleavage of S proteins by cathepsin L.[21,23,32] Furthermore, SARS-CoV-2 S1 itself enters host cells via receptor-mediated endocytosis.[12,46] We have shown that SARS-CoV-2 S1 enters endolysosomes in neuronal cells.[45] Using a concentration of 50 ng/mL that is present in the blood of COVID-19 patients,[50] we demonstrated that SARS-CoV-2 S1 induces endolysosome de-acidification in U87MG cells (Figure 1A), a finding that is consistent with our previous observation in neuronal cells.[45] An interesting observation from our previous study is that S1 protein from SARS-CoV, which is responsible for the 2002–2004 SARS outbreak, does not induce endolysosome de-acidification.[45] Because S1 protein from SARS-CoV lacks the multibasic motif, we suspect that the multibasic motif present on SARS-CoV-2 S1 may be responsible for its endolysosome de-acidifying effect. To test this, we determined the extent to which recombinant mutant SARS-CoV-2 S1 lacking the multibasic motif affects endolysosome pH in U87MG cells. We demonstrated that mutant S1 without the multibasic motif (RRAR) failed to increase endolysosome pH (Figure 1A). Thus, the multibasic motif is critical for SARS-CoV-2 S1-induced endolysosome de-acidification.

To assess whether the multibasic motif affects the binding of spike protein to cell surface ACE2 receptor, which mediates the internalization of spike protein, an ACE2: spike S1 RBD inhibitor screening assay was perform using various concentrations of S1 and mutant S1 lacking the multibasic motif. We demonstrated that S1 and mutant S1 lacking the multibasic motif exhibited similar inhibition on the binding of spike S1 RBD to ACE2 (Figure 1B). Thus, the multibasic motif may not affect SARS-CoV-2 S1-induced endolysosome de-acidification at cell surface. We speculate that the multibasic motif of SARS-CoV-2 S1 may interact with an endolysosome-resident protein, which mediates S1-induced endolysosome de-acidification effect. Interestingly, SLC38A9 has been shown to function as an endolysosome arginine sensor that interacts with v-ATPase, the proton pump that acidifies endolysosomes.[47–49] Thus, we speculate that SLC38A9 interacts with the multibasic motif of S1 and mediates S1-induced endolysosome de-acidification.

As an initial step to investigate such a possibility, we determined whether SARS-CoV-2 S1 and SLC38A9 could present in the same compartment inside the cell. We demonstrated that both fluorescent labeled SARS-CoV-2 S1 and SLC38A9-RFP were present in endolysosomes identified with LysoTracker (Figure 1C) in U87MG cells. Importantly, we demonstrated the co-localization of fluorescent labeled SARS-CoV-2 S1 with SLC38A9-RFP (Figure 1C). To further assess the physical interaction between SARS-CoV-2 S1 and SLC38A9, we utilized pull-down and/or immunoprecipitation method. Using biotin-labeled SARS-CoV-2 S1 proteins as bait proteins, SLC38A9 was pulled down from U87MG cell lysates (Figure 1D); and as a control, TLR3, an endolysosome-resident RNA sensor protein, was not pulled down (Figure 1D). In an immunoprecipitation assay, using SLC38A9 antibodies as bait proteins that pull down SLC38A9 from U87MG cell lysates, we also demonstrate the interaction between S1 and SLC38A9 (Figure 1E). However, we did not demonstrate a robust interaction between SLC38A9 and S1 lacking the multibasic motif (Figure 1F). Together, our findings suggest that the multibasic motif is critical for the interaction between SARS-CoV-2 S1 and SLC38A9.

SLC38A9 mediates SARS-CoV-2 S1-induced endolysosome de-acidification and dysfunction

Using SLC38A9 knockdown strategy, we tested further the hypothesis that SLC38A9 mediates S1-induced endolysosome de-acidification. In U87MG cells, we demonstrated the siRNA knockdown of SLC38A9 (Figure 2A) did not significantly affect basal levels of endolysosome pH (Figure 2B); however, SLC38A9 knockdown significantly blocked S1-induced endolysosome de-acidification (Figure 2B). As a functional outcome of endolysosome de-acidification, we checked the levels of active cathepsin D (CatD) in endolysosomes using the dye BODIPY FL-pepstatin A—a fluorescence-tagged cathepsin D inhibitor that binds to the active site of cathepsin D when its active site is open under acidic pH conditions. The percentage of active endolysosomes (active CatD positive) to total endolysosomes stained with LysoTracker red (LTR) decreased upon the addition of SARS-CoV-2 S1 at 50 ng/mL for 48 h in scramble siRNA treated U87MG cells (Figure 2C), and such an effect was blocked by SLC38A9 knockdown (Figure 2C). Thus, our findings suggest that SLC38A9 mediates SARS-CoV-2 S1-induced endolysosome de-acidification and dysfunction.

SLC38A9 knockdown attenuates SARS-CoV-2 viral entry

Endolysosomes form an integral part of the SARS-CoV-2 infection[51–53] including viral entry into host cells (Bayati et al., 2021; Koch et al., 2021) and egress from host cells (Ghosh et al., 2020). Given that endosomes/lysosomes are critical for the degradation of internalized SARS-CoV-2,[12] we addressed question of whether the endolysosome de-acidifying effect of S1 affects viral entry using a pseudoSARS-CoV-2 that enters the host cell via receptor-mediated endocytosis.[54] This pseudo-typed lentivirus with SARS-CoV-2 S protein as the envelope glycoproteins contains the luciferase gene driven by a CMV promoter. Thus, viral entry into host cells can be measured with luciferase activity assay.[55] Given our observation that SLC38A9 mediates S1-induced endolysosome de-acidification, we generated multiple

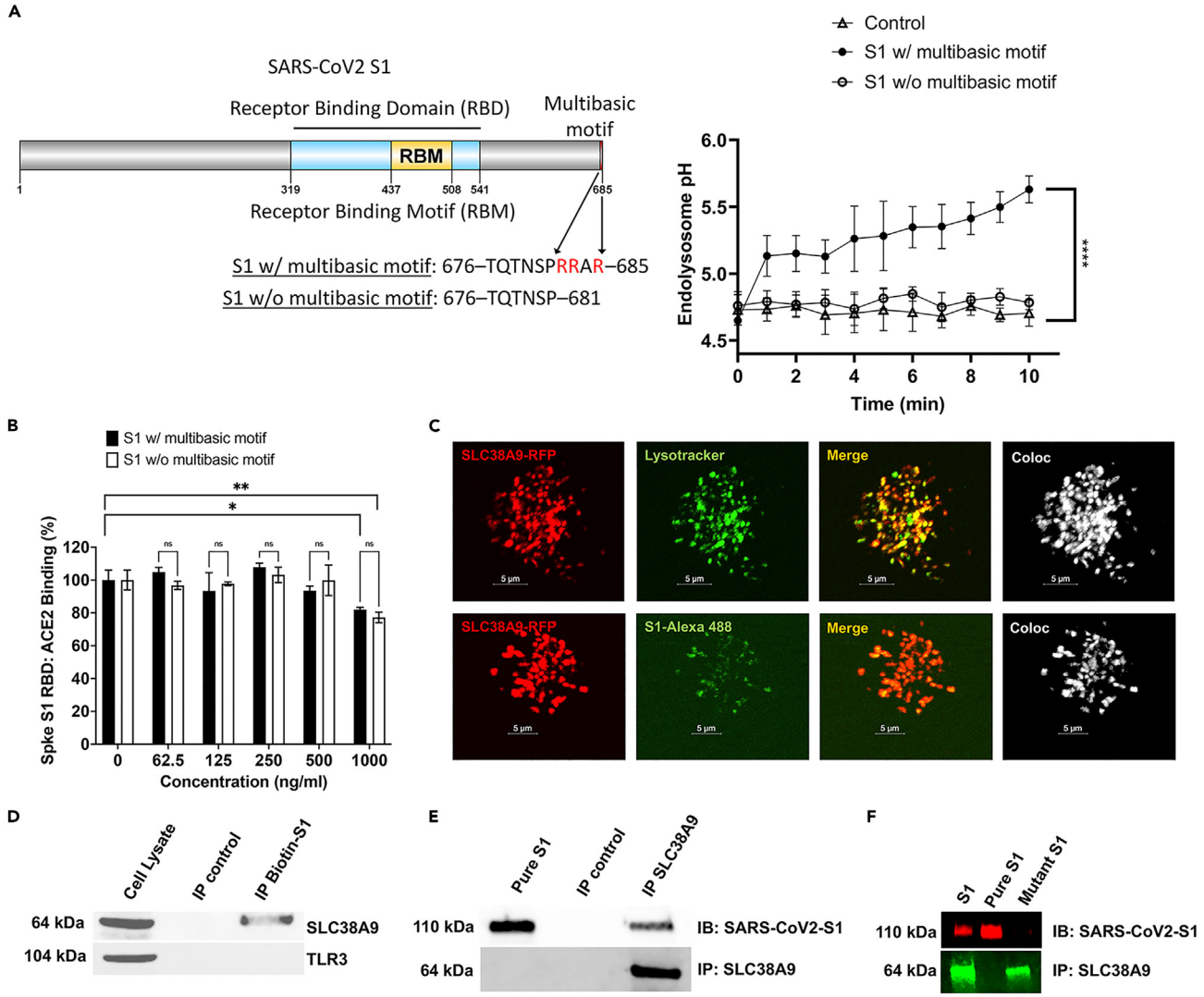

Figure 1. The multibasic motif of SARS-CoV-2 S1, which is critical for its endolysosome de-acidifying effect, interacts with SLC39A9

(A) Recombinant SARS-CoV-2 S1 (S1 w/multibasic motif, 50 ng/mL) but not mutant S1 lacking the multibasic motif (S1 w/o multibasic motif, 50 ng/mL), induces endolysosome de-acidification in U87MG cells ($n = 3$ repeats, ****$p < 0.0001$).

(B) S1w/multibasic motif and mutant S1 w/o multibasic motif exhibit similar inhibition on the binding of spike protein receptor binding domain to ACE2 ($n = 3$ repeats, *$p<0.05$, **$p<0.01$).

(C) Fluorescent labeled SARS-CoV-2 S1 co-localizes with SLC38A9-RFP in endolysosomes (LysoTracker) in U87MG cells (scale bar, 5 μm).

(D) Using biotin-labeled SARS-CoV-2 S1 proteins as bait proteins, SLC38A9, but not TLR3, was pulled down from U87MG cell lysates.

(E) Using SLC38A9 antibodies as bait proteins that pull down SLC38A9 from U87MG cell lysates, S1 was detected.

(F) Using SLC38A9 antibodies as bait proteins that pull down SLC38A9 from U87MG cell lysate, mutant S1 lacking the multibasic motif was not detected.

stable SLC38A9 knockdown cell lines (Figure 3). We determined effects of SLC38A9 knockdown on S protein-mediated entry of pseudo-SARS-CoV-2 in U87MG human glioblastoma cells (Figure 3A), Calu-3 human lung adenocarcinoma cells (Figure 3B), Caco-2 human colorectal adenocarcinoma cells (Figure 3C), and A549 human lung adenocarcinoma cells (Figure 3D). In all these cells, we demonstrated that SLC38A9 knockdown significantly attenuated S protein-mediated pseudo-SARS-CoV-2 entry as indicated by decreases in luciferase activity, without affecting protein levels of ACE2 (data not shown). Our findings suggest that multibasic motif (RRAR)-dependent interaction with SLC38A9 is critical for pseudo-SARS-CoV-2 entry. Given that SARS-CoV-1 S proteins do not have the multibasic motif as that of SARS-CoV-2 S, SLC38A9 knockdown should not affect the SARS-CoV-1 viral entry. Using a luciferase-base pseudoSARS-CoV-1 virus, we determined the effect of SLC38A9 knockdown on pseudoSARS-CoV-1 viral entry. As expected, SLC38A9 knockdown did not affect SARS-CoV-1 viral entry in U87MG cells (Figure 3E). Such a finding support further the important role of multibasic motif (RRAR)-dependent interaction with SLC38A9 plays in SARS-CoV-2 entry. To further assess the possibility that SARS-CoV-2 S1 in endolysosomes could enhance viral entry,

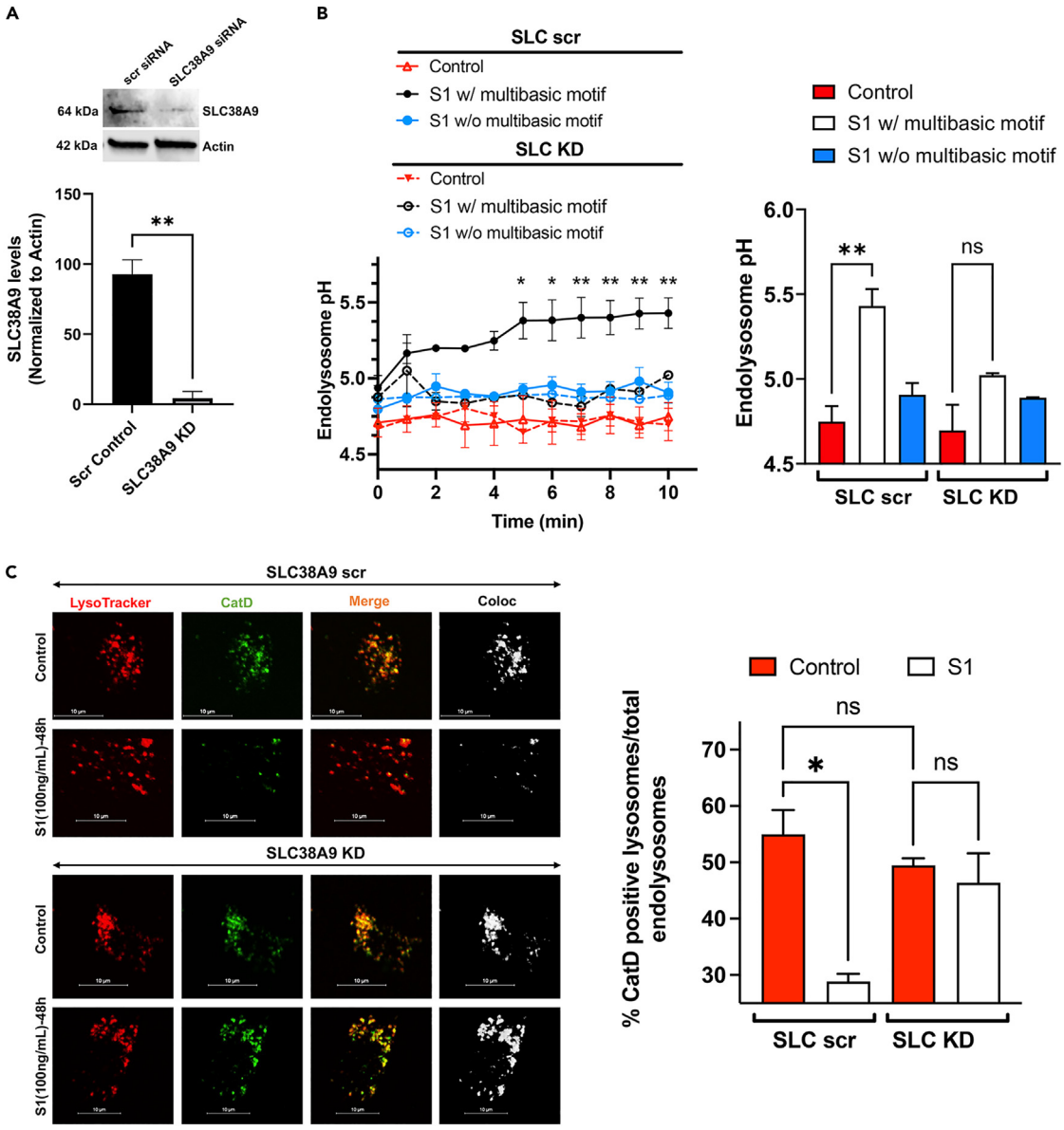

Figure 2. SLC38A9 knockdown prevents SARS-CoV-2 S1-induced endolysosome de-acidification and dysfunction

(A) Immunoblotting shows the siRNA knockdown of SLC38A9 in U87MG cells (n = 3 repeats, $^{**}p < 0.01$).

(B) SLC38A9 knockdown significantly blocked S1-induced endolysosome de-acidification (line graph). Bar-graph shows changes of endolysosome pH at 10-min timepoint following S1 treatment (n = 3 repeats, $^{*}p<0.05$, $^{**}p < 0.01$, ns $p>0.05$).

(C) SARS-CoV-2 S1 (50 ng/mL for 48 h) significantly decreased the percentage of active endolysosomes (CatD positive vs. total endolysosomes) in scramble siRNA treated U87MG cells (scale bar, 10 μm), but not in SLC38A9 knockdown cells (n = 3 repeats, $^{*}p < 0.05$, ns $p>0.05$).

we determined dose response of SARS-CoV-2 S1 (0.1, 1, 10, 100, and 200 ng/mL) on S protein-mediated pseudoSARS-CoV-2 viral entry in U87MG cells. In this study, S1 proteins were applied to the U87MG cells for 2 h, after which S1 proteins were washed out and cells were incubated with pseudoSARS-CoV-2 for 48 h followed by luciferase activity assay. We demonstrated that S1 at the concentrations of 1 ng/mL and above significantly enhanced SARS-CoV-2 viral entry (Figure 3F), with S1 at the concentration of 100 ng/mL having the maximal effect and the enhancing effect of S1 on SARS-CoV-2 viral entry being reduced at the concentration of 200 ng/mL. Given that SARS-CoV-1 S1 proteins do not exert endolysosome de-acidification as that of SARS-CoV-2 S1,[45] we speculate that SARS-CoV-1 S1 may not exert enhancing effect on viral entry as that of SARS-CoV-2 S1. Thus, we determined dose response of SARS-CoV-1 S1 (0.1, 1, 10, 100, and 200 ng/mL) on S protein-mediated pseudoSARS-CoV-1 viral entry in U87MG cells using the same strategy described previously. As expected, SARS-CoV-1 S1 did not significantly affect SARS-CoV-1 viral entry (Figure 3G).

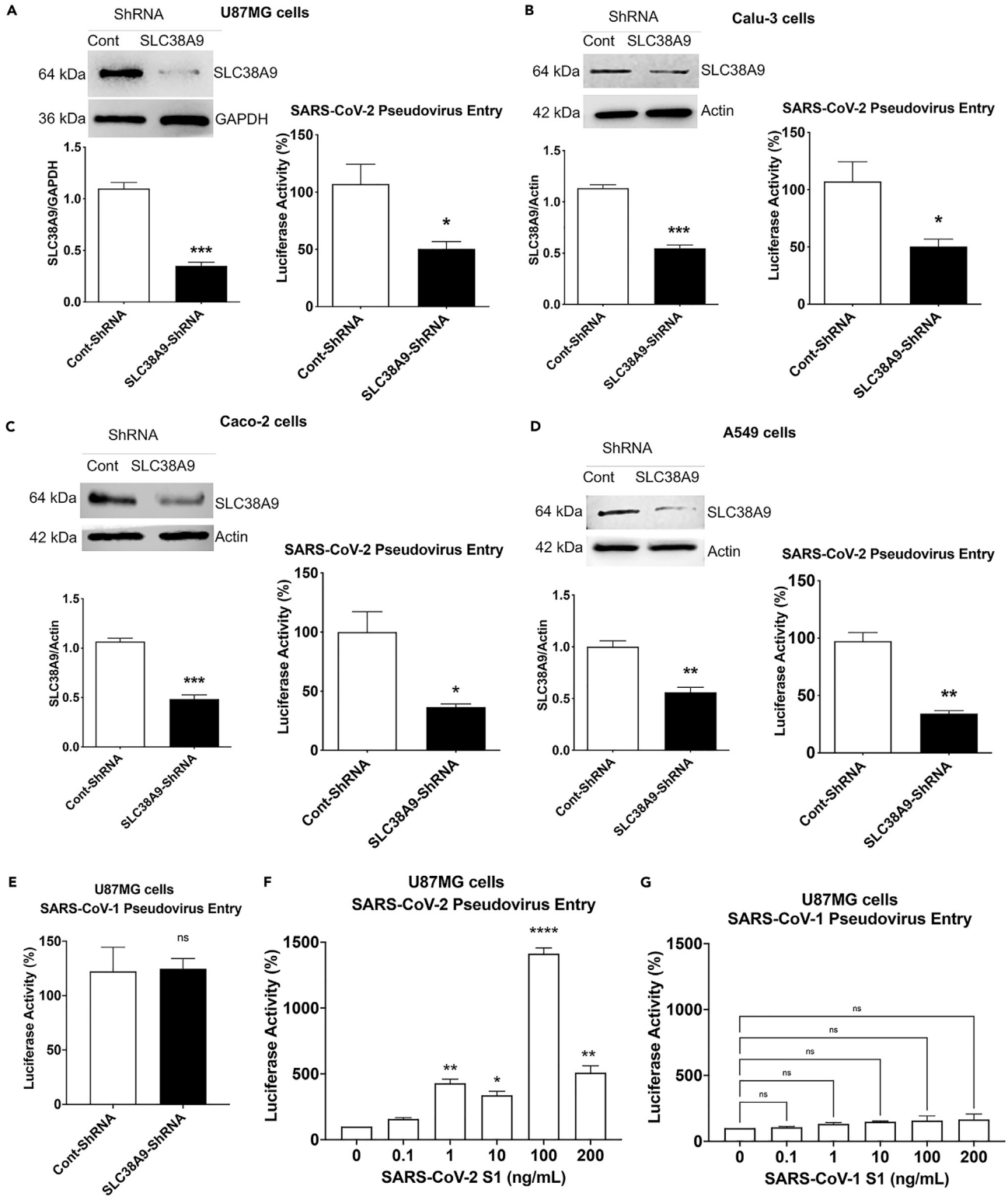

Figure 3. SLC38A9 knockdown blocks SARS-CoV-2 viral entry

(A–D) SLC38A9 knockdown attenuated S protein-mediated entry of pseudo-SARS-CoV-2 as indicated by decreases in luciferase activity in U87MG human glioblastoma cells (A), Calu-3 human lung adenocarcinoma cells (B), Caco-2 human colorectal adenocarcinoma cells (C), and A549 human lung adenocarcinoma cells (D) ($n = 3$ repeats, $^{*}p < 0.05$, $^{**}p < 0.01$, $^{***}p < 0.001$).

Figure 3. *Continued*

(E) SLC38A9 knockdown did not affect S protein-mediated entry of pseudo-SARS-CoV-1 in U87MG cells ($n = 2$ repeats, ns $p > 0.05$).

(F) SARS-CoV-2 S1 treatment at the concentration of 1 ng/mL and above significantly enhanced SARS-CoV-2 viral entry in U87MG cells ($n = 2$ repeats, *$p < 0.05$, **$p < 0.01$, ****$p < 0.0001$).

(G) SARS-CoV-1 S1 treatment did not significantly affect SARS-CoV-1 viral entry in U87MG cells ($n = 2$ repeats, ns $p > 0.05$).

DISCUSSION

The prominent findings reported here are that the multibasic motif of SARS-CoV-2 S1 is critical for its interaction with SLC38A9, that SLC38A9 knockdown prevents S1-induced endolysosome de-acidification, and that SLC38A9 knockdown blocks S protein-mediated entry of pseudo-SARS-CoV-2.

Endolysosomes are acidic organelles that are responsible for degrading materials derived from endocytic pathway and autophagic pathway.[56] Endolysosomes contain up to 60 acid hydrolytic enzymes including proteases, lipases, and nucleases,[56] and these hydrolases are not only critical for maintaining cellular homeostasis but also important for degradation of pathogens including SARS-CoV-2[12,57] and HIV-1[58,59], HSV-1,[60] Zika virus, and[61] HBV.[62] Recent genome-wide CRISPR screen studies indicate that endolysosomes form an integral part of the SARS-CoV-2 infection.[51–53] Indeed, endolysosomes contribute to SARS-CoV-2 viral entry into[12,34] and egress[63] from host cells. In the step of viral entry, upon entering endolysosomes via receptor-mediated endocytosis,[12,37] cleavage of S protein would occur in endolysosomes by pH-sensitive endolysosome-resident cathepsin L.[42,43] Such a proteolytic cleavage of SARS-CoV-2 S protein in endolysosomes could result in dissociation of S1 from viral envelope and exposure of fusion peptide on S2 subunit, which enables the fusion of viral membrane with endolysosomes membrane[26,27] and the release of viral RNA into the cytosol where viral replication occurs.[30,31]

If endolysosome-resident pH-sensitive hydrolytic enzymes can cleave S protein, up to 60 other endolysosome-resident acid hydrolytic enzymes including proteases, lipases, and nucleases should have the ability to completely degrade internalized SARS-CoV-2 virus, and the chance of S2-mediated fusion with endolysosome membrane occurring should be slim. However, SARS-CoV-2 residing in endolysosomes manages to subvert the endosomal system, overcome the complete degradation by up to 60 acid hydrolytic enzymes, and measurable viral entry via endolysosomes does occur.[12,34] Findings from our present study provide a novel mechanism by which SARS-CoV-2 could escape complete degradation by 60 endolysosome-resident acid hydrolytic enzymes.

S1 can present in the lumen of endolysosome via two different mechanisms. First, dissociated S1 containing the multibasic motif can enter host cell endosomes via receptor-mediated endocytosis.[12,45,46] Second, SARS-CoV-2 virus can be internalized into endolysosome, where proteolytic cleavage of S proteins by cathepsin L can result in the release of S1 from viral envelope and the exposure of a multibasic motif on S1.[24,25] This multibasic motif of S1 in endolysosomes could interact with SLC38A9, which is an endolysosome arginine sensor that interacts with vacuolar ATPase[47–49] and induces endolysosome de-acidification.[45] Indeed, we have demonstrated that the multibasic motif of SARS-CoV-2 S1 is critical for its interaction with SLC38A9 and that SLC38A9 knockdown prevents S1-mediated endolysosome de-acidification and dysfunction. Such S1-mediated endolysosome de-acidification should prevent complete degradation of internalized SARS-CoV-2 by up to 60 acid hydrolytic enzymes and enhance the chance of S2-mediated fusion with endolysosome membrane and the release of viral RNA into the cytosol for viral replication. It should be noted that one single SARS-CoV-2 virion can generate up to 300 monomeric S1.[64] Thus, even if only one or a very few virions are present in endosomes, significant amount of S1 proteins could be generated at the site of endolysosomes, which could induce endolysosome de-acidification via multibasic motif (RRAR)-dependent interaction with SLC38A9, giving the virions more time to remain intact within lumens before enacting virus-cell membrane fusion. Furthermore, we have demonstrated that externally added S1 proteins exert pro-viral effect and enhance the entry of pseudo-SARS-CoV-2 in to U87MG cells.

Thus, blocking SLC38A9 should attenuate SARS-CoV-2 viral entry. Excitingly, we have demonstrated that SLC38A9 knockdown attenuates S protein-mediated entry of pseudo-SARS-CoV-2 in various cells including Calu-3, U87MG, Caco-2, and A549 cells. Although such findings need to be confirmed with live SARS-CoV-2 virus, our findings are supported by others' findings showing that the lack of the multibasic motif impairs SARS-CoV-2 viral entry into the host cells[15,24] and decreases SARS-CoV-2 viral infection and transmission in animal models.[53,65] Furthermore, such SLC38A9-mediated S1-induced endolysosome de-acidification and dysfunction could contribute to the persistence of SARS-CoV-2 virus[3–6] that contributes to the development of long COVID.

It should be noted that the presence of such a multibasic motif (RRAR) distinguishes SARS-CoV-2 from SARS-CoV-1 that causes SARS outbreak in 2002–2004 and all other known sarbecoviruses whose S protein is not cleaved by furin proteases.[23–25,28] Furthermore, such an multibasic motif is present in the envelope protein of many other highly infectious viruses including influenza virus H5A1, Ebola virus, Zika virus, and HIV-1.[66] Like SARS-CoV-2, many of these deadly viruses, such as Ebola,[67] HIV-1[58,59], Zika virus,[61] and influenza,[68,69] can infect host cell by fusion of viral membrane with endolysosomes membrane and the release of viral genome into the cytosol for replication.[70] Yet, they all have the ability to subvert the endosomal system and escape the degradation by up to 60 acid hydrolytic enzymes in endolysosomes.

The acidic pH in endolysosomes and/or proteolytic processing of their envelope proteins by endolysosomal enzymes are needed for enveloped viral entry into host cells; as such lysosomotropic agents such chloroquine (CQ) and hydroxychloroquine (HCQ), which are diprotic weak base drugs that preferentially enter acidic endolysosomes and neutralize their luminal pH,[71,72] have been proposed as antiviral agents against influenza A, HIV-1, and SARS-CoV-2. Although CQ can inhibit influenza A *in vitro*,[73,74] CQ was ineffective against influenza infection when tested using *in vivo* animal models[75] or in human clinical trials.[76] Similarly, CQ and HCQ suppressed HIV-1 replication *in vitr*[77] but showed mixed results when tested clinically in human populations.[78–80] Worse, recent studies reported that CQ increased HIV-1 viremia.[81,82]

At the beginning of COVID-19 outbreak, pH-dependent SARS-CoV-2 viral entry has provided rationale for testing CQ and HCQ as antiviral agents against SARS-CoV-2. Early *in vitro* evidence indicated that CQ inhibited the ability of SARS-CoV-2 to infect monkey kidney-derived Vero E6 cells.[83–85] However, such antiviral effects of CQ were not replicated in human lung cells,[86] which is consistent with clinical studies showing that CQ and HCQ had no therapeutic effect on COVID-19 patients[87–89] and even had worsened outcomes.[90,91] Thus, de-acidifying endolysosomes with CQ and HCQ does not represent a good antiviral strategy.

The acidic environment of endolysosomes is also critical for the degradation of internalized viruses such as SARS-CoV-2[12] and HIV-1.[58] As such, de-acidifying endolysosomes with CQ or HCQ could impair host cell's ability to degrade invading viruses. Consistent with this notion, we have demonstrated that externally added S1 proteins, which induce endolysosome de-acidification, exert pro-viral effect and enhance the entry of pseudo-SARS-CoV-2 into U87MG cells. In contrast to de-acidifying endolysosomes, we speculate that acidifying endolysosomes represent a promising therapy against COVID-19, as acidifying endolysosomes could enhance many lysosomal hydrolases with optimal proteolytic activity at in more acidic environment (pH 3–5), thus facilitating the complete degradation of internalized SARS-CoV-2 and reducing the chance of S2-mediated fusion and viral entry into host cell. Furthermore, it should be noted that cathepsin L, the enzyme involved in the cleavage of S proteins in endolysosomes, is activated at pH ~5.5–6 and has an optimal proteolytic activity in slightly acidic environment. More importantly, cathepsin L is irreversibly inactivated at pH < 4.[92] Thus, endolysosome acidification could decrease cathepsin L activity and exert antiviral effect. Indeed, our published findings demonstrate that acidifying endolysosomes reduces pseudoSARS-CoV-2 entry into host cell.[55] Consistently, findings from our current study have demonstrated that SLC38A9 knockdown, which prevents S1-induced endolysosome de-acidification, attenuates S protein-mediated entry of pseudo-SARS-CoV-2.

In summary, our findings provide a novel mechanism in regulating SARS-CoV-2 viral entry; S1 in the lumen of endolysosomes could interact with SLC38A9, which leads to endolysosome de-acidification and dysfunction, contributing to the escape of SARS-CoV-2 from endolysosomes and enhancing viral entry. Our findings also suggest that SLC38A9 represents as a novel therapeutic target for the treatment of COVD-19.

Limitations of the study

This study has uncovered a novel mechanism whereby released S1 regulates SARS-CoV-2 viral entry. Releasable S1 protein contains a multi-basic motif with multiple arginine on its C-terminus of S1. Upon entering host cell endolysosomes, S1 interacts with an endolysosome resident arginine-rich sensor SLC38A9 and induces endolysosome de-acidification and dysfunction, facilitating the escape of SARS-CoV-2 from endolysosomes and enhancing viral entry. A limitation of the present study is that such findings are based on studies conducted in human cell lines using pseudo-SARS-CoV-2. Our findings need to be confirmed with live SARS-CoV-2 virus in primary human cells.

STAR★METHODS

Detailed methods are provided in the online version of this paper and include the following:

- KEY RESOURCES TABLE
- RESOURCE AVAILABILITY
  - Lead contact
  - Materials availability
  - Data and code availability
- EXPERIMENTAL MODEL AND STUDY PARTICIPANT DETAILS
  - Cells
- METHOD DETAILS
  - Pulldown and immunoprecipitation
  - The spike-ACE2 binding assay
  - siRNA knockdown
  - Generating SLC38A9 knockdown stable cell line
  - Endolysosome pH measurement
  - Active cathepsin D staining
  - Cellular entry of SARS-CoV-2 spike protein pseudo-virus
  - Cellular entry of SARS-CoV-1 spike protein pseudo-virus
  - SLC38A9-RFP expression
  - Live cell imaging
  - Immunoblotting
- QUANTIFICATION AND STATISTICAL ANALYSIS

ACKNOWLEDGMENTS

This work was supported by the National Institute of Mental Health [MH119000], National Institute of Mental Health [MH134592], National Institute on Drug Abuse [DA059280].

AUTHOR CONTRIBUTIONS

G.D., N.K., and X.C. designed the research. G.D., N.R., W.H., and N.K. performed experiments and analyzed data. G.D. and X.C. wrote the manuscript.

DECLARATION OF INTERESTS

The authors declare no competing interests.

Received: March 4, 2024
Revised: May 13, 2024
Accepted: June 24, 2024
Published: June 27, 2024

REFERENCES

1. Shereen, M.A., Khan, S., Kazmi, A., Bashir, N., and Siddique, R. (2020). COVID-19 infection: Origin, transmission, and characteristics of human coronaviruses. J. Adv. Res. *24*, 91–98. https://doi.org/10.1016/j.jare.2020.03.005.
2. Wang, C., Horby, P.W., Hayden, F.G., and Gao, G.F. (2020). A novel coronavirus outbreak of global health concern. Lancet *395*, 470–473. https://doi.org/10.1016/S0140-6736(20)30185-9.
3. Lee, M.H., Perl, D.P., Nair, G., Li, W., Maric, D., Murray, H., Dodd, S.J., Koretsky, A.P., Watts, J.A., Cheung, V., et al. (2021). Microvascular Injury in the Brains of Patients with Covid-19. N. Engl. J. Med. *384*, 481–483. https://doi.org/10.1056/NEJMc2033369.
4. Lee, M.H., Perl, D.P., Steiner, J., Pasternack, N., Li, W., Maric, D., Safavi, F., Horkayne-Szakaly, I., Jones, R., Stram, M.N., et al. (2022). Neurovascular injury with complement activation and inflammation in COVID-19. Brain *145*, 2555–2568. https://doi.org/10.1093/brain/awac151.
5. Stein, S.R., Ramelli, S.C., Grazioli, A., Chung, J.Y., Singh, M., Yinda, C.K., Winkler, C.W., Sun, J., Dickey, J.M., Ylaya, K., et al. (2022). SARS-CoV-2 infection and persistence in the human body and brain at autopsy. Nature *612*, 758–763. https://doi.org/10.1038/s41586-022-05542-y.
6. Bussani, R., Zentilin, L., Correa, R., Colliva, A., Silvestri, F., Zacchigna, S., Collesi, C., and Giacca, M. (2023). Persistent SARS-CoV-2 infection in patients seemingly recovered from COVID-19. J. Pathol. *259*, 254–263. https://doi.org/10.1002/path.6035.
7. Swank, Z., Senussi, Y., Manickas-Hill, Z., Yu, X.G., Li, J.Z., Alter, G., and Walt, D.R. (2023). Persistent Circulating Severe Acute Respiratory Syndrome Coronavirus 2 Spike Is Associated With Post-acute Coronavirus Disease 2019 Sequelae. Clin. Infect. Dis. *76*, e487–e490. https://doi.org/10.1093/cid/ciac722.
8. Craddock, V., Mahajan, A., Spikes, L., Krishnamachary, B., Ram, A.K., Kumar, A., Chen, L., Chalise, P., and Dhillon, N.K. (2023). Persistent circulation of soluble and extracellular vesicle-linked Spike protein in individuals with postacute sequelae of COVID-19. J. Med. Virol. *95*, e28568. https://doi.org/10.1002/jmv.28568.
9. Crunfli, F., Carregari, V.C., Veras, F.P., Vendramini, P.H., Valença, A.G.F., Antunes, A.S.L.M., Brandão-Teles, C., da Silva Zuccoli, G., Reis-de-Oliveira, G., Silva-Costa, L.C., et al. (2022). Morphological, cellular and molecular basis of brain infection in COVID-19 patients. Preprint at medRxiv *95*, e28568. https://doi.org/10.1101/2020.10.09.20207464.
10. Yang, C., Zhao, H., Espín, E., and Tebbutt, S.J. (2023). Association of SARS-CoV-2 infection and persistence with long COVID. Lancet Respir. Med. *11*, 504–506. https://doi.org/10.1016/S2213-2600(23)00142-X.
11. Ford, N.D., Slaughter, D., Edwards, D., Dalton, A., Perrine, C., Vahratian, A., and Saydah, S. (2023). Long COVID and Significant Activity Limitation Among Adults, by Age - United States, June 1-13, 2022, to June 7-19, 2023. MMWR Morb. Mortal. Wkly. Rep. *72*, 866–870. https://doi.org/10.15585/mmwr.mm7232a3.
12. Bayati, A., Kumar, R., Francis, V., and McPherson, P.S. (2021). SARS-CoV-2 infects cells after viral entry via clathrin-mediated endocytosis. J. Biol. Chem. *296*, 100306. https://doi.org/10.1016/j.jbc.2021.100306.
13. Jackson, C.B., Farzan, M., Chen, B., and Choe, H. (2022). Mechanisms of SARS-CoV-2 entry into cells. Nat. Rev. Mol. Cell Biol. *23*, 3–20. https://doi.org/10.1038/s41580-021-00418-x.
14. Yan, R., Zhang, Y., Li, Y., Xia, L., Guo, Y., and Zhou, Q. (2020). Structural basis for the recognition of SARS-CoV-2 by full-length human ACE2. Science *367*, 1444–1448. https://doi.org/10.1126/science.abb2762.
15. Cantuti-Castelvetri, L., Ojha, R., Pedro, L.D., Djannatian, M., Franz, J., Kuivanen, S., van der Meer, F., Kallio, K., Kaya, T., Anastasina, M., et al. (2020). Neuropilin-1 facilitates SARS-CoV-2 cell entry and infectivity. Science *370*, 856–860. https://doi.org/10.1126/science.abd2985.
16. Daly, J.L., Simonetti, B., Klein, K., Chen, K.E., Williamson, M.K., Antón-Plágaro, C., Shoemark, D.K., Simón-Gracia, L., Bauer, M., Hollandi, R., et al. (2020). Neuropilin-1 is a host factor for SARS-CoV-2 infection. Science *370*, 861–865. https://doi.org/10.1126/science.abd3072.
17. Wang, K., Chen, W., Zhang, Z., Deng, Y., Lian, J.Q., Du, P., Wei, D., Zhang, Y., Sun, X.X., Gong, L., et al. (2020). CD147-spike protein is a novel route for SARS-CoV-2 infection to host cells. Signal Transduct. Target. Ther. *5*, 283. https://doi.org/10.1038/s41392-020-00426-x.
18. Belouzard, S., Chu, V.C., and Whittaker, G.R. (2009). Activation of the SARS coronavirus spike protein via sequential proteolytic cleavage at two distinct sites. Proc. Natl. Acad. Sci. USA *106*, 5871–5876. https://doi.org/10.1073/pnas.0809524106.
19. Takeda, M. (2022). Proteolytic activation of SARS-CoV-2 spike protein. Microbiol. Immunol. *66*, 15–23. https://doi.org/10.1111/1348-0421.12945.
20. Matsuyama, S., Nagata, N., Shirato, K., Kawase, M., Takeda, M., and Taguchi, F. (2010). Efficient activation of the severe acute respiratory syndrome coronavirus spike protein by the transmembrane protease TMPRSS2. J. Virol. *84*, 12658–12664. https://doi.org/10.1128/JVI.01542-10.
21. Ou, T., Mou, H., Zhang, L., Ojha, A., Choe, H., and Farzan, M. (2021). Hydroxychloroquine-mediated inhibition of SARS-CoV-2 entry is attenuated by TMPRSS2. PLoS Pathog. *17*, e1009212. https://doi.org/10.1371/journal.ppat.1009212.
22. Ozono, S., Zhang, Y., Ode, H., Sano, K., Tan, T.S., Imai, K., Miyoshi, K., Kishigami, S., Ueno, T., Iwatani, Y., et al. (2021). SARS-CoV-2 D614G spike mutation increases entry efficiency with enhanced ACE2-binding affinity. Nat. Commun. *12*, 848. https://doi.org/10.1038/s41467-021-21118-2.
23. Hoffmann, M., Kleine-Weber, H., Schroeder, S., Krüger, N., Herrler, T., Erichsen, S., Schiergens, T.S., Herrler, G., Wu, N.H., Nitsche, A., et al. (2020). SARS-CoV-2 Cell Entry Depends on ACE2 and TMPRSS2 and Is Blocked by a Clinically Proven Protease Inhibitor. Cell *181*, 271–280.e8. https://doi.org/10.1016/j.cell.2020.02.052.
24. Hoffmann, M., Kleine-Weber, H., and Pohlmann, S. (2020). A Multibasic Cleavage Site in the Spike Protein of SARS-CoV-2 Is Essential for Infection of Human Lung Cells. Mol Cell *78*, 779–784.e775. https://doi.org/10.1016/j.molcel.2020.04.022.
25. Shang, J., Wan, Y., Luo, C., Ye, G., Geng, Q., Auerbach, A., and Li, F. (2020). Cell entry mechanisms of SARS-CoV-2. Proc. Natl. Acad. Sci. USA *117*, 11727–11734. https://doi.org/10.1073/pnas.2003138117.
26. Fan, X., Cao, D., Kong, L., and Zhang, X. (2020). Cryo-EM analysis of the post-fusion structure of the SARS-CoV spike glycoprotein. Nat. Commun. *11*, 3618. https://doi.org/10.1038/s41467-020-17371-6.
27. Walls, A.C., Tortorici, M.A., Snijder, J., Xiong, X., Bosch, B.J., Rey, F.A., and Veesler, D. (2017). Tectonic conformational changes of a coronavirus spike glycoprotein promote membrane fusion. Proc. Natl. Acad. Sci. USA *114*, 11157–11162. https://doi.org/10.1073/pnas.1708727114.
28. Ou, X., Liu, Y., Lei, X., Li, P., Mi, D., Ren, L., Guo, L., Guo, R., Chen, T., Hu, J., et al. (2020). Characterization of spike glycoprotein of SARS-CoV-2 on virus entry and its immune cross-reactivity with SARS-CoV. Nat.

Commun. *11*, 1620. https://doi.org/10.1038/s41467-020-15562-9.

29. Peng, R., Wu, L.A., Wang, Q., Qi, J., and Gao, G.F. (2021). Cell entry by SARS-CoV-2. Trends Biochem. Sci. *46*, 848–860. https://doi.org/10.1016/j.tibs.2021.06.001.
30. Xia, S., Zhu, Y., Liu, M., Lan, Q., Xu, W., Wu, Y., Ying, T., Liu, S., Shi, Z., Jiang, S., and Lu, L. (2020). Fusion mechanism of 2019-nCoV and fusion inhibitors targeting HR1 domain in spike protein. Cell. Mol. Immunol. *17*, 765–767. https://doi.org/10.1038/s41423-020-0374-2.
31. Schaefer, S.L., Jung, H., and Hummer, G. (2021). Binding of SARS-CoV-2 Fusion Peptide to Host Endosome and Plasma Membrane. J. Phys. Chem. B *125*, 7732–7741. https://doi.org/10.1021/acs.jpcb.1c04176.
32. Peacock, T.P., Goldhill, D.H., Zhou, J., Baillon, L., Frise, R., Swann, O.C., Kugathasan, R., Penn, R., Brown, J.C., Sanchez-David, R.Y., et al. (2021). The furin cleavage site in the SARS-CoV-2 spike protein is required for transmission in ferrets. Nat. Microbiol. *6*, 899–909. https://doi.org/10.1038/s41564-021-00908-w.
33. Li, Z.L., and Buck, M. (2021). Neuropilin-1 assists SARS-CoV-2 infection by stimulating the separation of Spike protein S1 and S2. Biophys. J. *120*, 2828–2837. https://doi.org/10.1016/j.bpj.2021.05.026.
34. Koch, J., Uckeley, Z.M., Doldan, P., Stanifer, M., Boulant, S., and Lozach, P.Y. (2021). TMPRSS2 expression dictates the entry route used by SARS-CoV-2 to infect host cells. EMBO J. *40*, e107821. https://doi.org/10.15252/embj.2021107821.
35. Liu, J., Li, Y., Liu, Q., Yao, Q., Wang, X., Zhang, H., Chen, R., Ren, L., Min, J., Deng, F., et al. (2021). SARS-CoV-2 cell tropism and multiorgan infection. Cell Discov. *7*, 17. https://doi.org/10.1038/s41421-021-00249-2.
36. Li, F., Han, M., Dai, P., Xu, W., He, J., Tao, X., Wu, Y., Tong, X., Xia, X., Guo, W., et al. (2021). Distinct mechanisms for TMPRSS2 expression explain organ-specific inhibition of SARS-CoV-2 infection by enzalutamide. Nat. Commun. *12*, 866. https://doi.org/10.1038/s41467-021-21171-x.
37. Bugatti, A., Filippini, F., Bardelli, M., Zani, A., Chiodelli, P., Messali, S., Caruso, A., and Caccuri, F. (2022). SARS-CoV-2 Infects Human ACE2-Negative Endothelial Cells through an $\alpha_v\beta_3$ Integrin-Mediated Endocytosis Even in the Presence of Vaccine-Elicited Neutralizing Antibodies. Viruses *14*, 705. https://doi.org/10.3390/v14040705.
38. Junqueira, C., Crespo, Â., Ranjbar, S., de Lacerda, L.B., Lewandrowski, M., Ingber, J., Parry, B., Ravid, S., Clark, S., Schrimpf, M.R., et al. (2022). FcγR-mediated SARS-CoV-2 infection of monocytes activates inflammation. Nature *606*, 576–584. https://doi.org/10.1038/s41586-022-04702-4.
39. Maemura, T., Kuroda, M., Armbrust, T., Yamayoshi, S., Halfmann, P.J., and Kawaoka, Y. (2021). Antibody-Dependent Enhancement of SARS-CoV-2 Infection Is Mediated by the IgG Receptors FcγRIIA and FcγRIIIA but Does Not Contribute to Aberrant Cytokine Production by Macrophages. mBio *12*, e0198721. https://doi.org/10.1128/mBio.01987-21.
40. Wang, Z., Deng, T., Zhang, Y., Niu, W., Nie, Q., Yang, S., Liu, P., Pei, P., Chen, L., Li, H., and Cao, B. (2022). ACE2 can act as the secondary receptor in the FcγR-dependent ADE of SARS-CoV-2 infection. iScience *25*, 103720. https://doi.org/10.1016/j.isci.2021.103720.
41. Okuya, K., Hattori, T., Saito, T., Takadate, Y., Sasaki, M., Furuyama, W., Marzi, A., Ohiro, Y., Konno, S., Hattori, T., and Takada, A. (2022). Multiple Routes of Antibody-Dependent Enhancement of SARS-CoV-2 Infection. Microbiol. Spectr. *10*, e0155321. https://doi.org/10.1128/spectrum.01553-21.
42. Zhao, M.M., Zhu, Y., Zhang, L., Zhong, G., Tai, L., Liu, S., Yin, G., Lu, J., He, Q., Li, M.J., et al. (2022). Novel cleavage sites identified in SARS-CoV-2 spike protein reveal mechanism for cathepsin L-facilitated viral infection and treatment strategies. Cell Discov. *8*, 53. https://doi.org/10.1038/s41421-022-00419-w.
43. Jaimes, J.A., Millet, J.K., and Whittaker, G.R. (2020). Proteolytic Cleavage of the SARS-CoV-2 Spike Protein and the Role of the Novel S1/S2 Site. iScience *23*, 101212. https://doi.org/10.1016/j.isci.2020.101212.
44. George, S., Pal, A.C., Gagnon, J., Timalsina, S., Singh, P., Vydyam, P., Munshi, M., Chiu, J.E., Renard, I., Harden, C.A., et al. (2021). Evidence for SARS-CoV-2 Spike Protein in the Urine of COVID-19 patients. Preprint at medRxiv *95*, e28568. https://doi.org/10.1101/2021.01.27.21250637.
45. Datta, G., Miller, N.M., Halcrow, P.W., Khan, N., Colwell, T., Geiger, J.D., and Chen, X. (2021). SARS-CoV-2 S1 Protein Induces Endolysosome Dysfunction and Neuritic Dystrophy. Front. Cell. Neurosci. *15*, 777738. https://doi.org/10.3389/fncel.2021.777738.
46. Gorshkov, K., Susumu, K., Chen, J., Xu, M., Pradhan, M., Zhu, W., Hu, X., Breger, J.C., Wolak, M., and Oh, E. (2020). Quantum Dot-Conjugated SARS-CoV-2 Spike Pseudo-Virions Enable Tracking of Angiotensin Converting Enzyme 2 Binding and Endocytosis. ACS Nano *14*, 12234–12247. https://doi.org/10.1021/acsnano.0c05975.
47. Wyant, G.A., Abu-Remaileh, M., Wolfson, R.L., Chen, W.W., Freinkman, E., Danai, L.V., Vander Heiden, M.G., and Sabatini, D.M. (2017). mTORC1 Activator SLC38A9 Is Required to Efflux Essential Amino Acids from Lysosomes and Use Protein as a Nutrient. Cell *171*, 642–654.e12. https://doi.org/10.1016/j.cell.2017.09.046.
48. Wang, S., Tsun, Z.Y., Wolfson, R.L., Shen, K., Wyant, G.A., Plovanich, M.E., Yuan, E.D., Jones, T.D., Chantranupong, L., Comb, W., et al. (2015). Metabolism. Lysosomal amino acid transporter SLC38A9 signals arginine sufficiency to mTORC1. Science *347*, 188–194. https://doi.org/10.1126/science.1257132.
49. Savini, M., Zhao, Q., and Wang, M.C. (2019). Lysosomes: Signaling Hubs for Metabolic Sensing and Longevity. Trends Cell Biol. *29*, 876–887. https://doi.org/10.1016/j.tcb.2019.08.008.
50. Ogata, A.F., Maley, A.M., Wu, C., Gilboa, T., Norman, M., Lazarovits, R., Mao, C.P., Newton, G., Chang, M., Nguyen, K., et al. (2020). Ultra-Sensitive Serial Profiling of SARS-CoV-2 Antigens and Antibodies in Plasma to Understand Disease Progression in COVID-19 Patients with Severe Disease. Clin. Chem. *66*, 1562–1572. https://doi.org/10.1093/clinchem/hvaa213.
51. Baggen, J., Persoons, L., Vanstreels, E., Jansen, S., Van Looveren, D., Boeckx, B., Geudens, V., De Man, J., Jochmans, D., Wauters, J., et al. (2021). Genome-wide CRISPR screening identifies TMEM106B as a proviral host factor for SARS-CoV-2. Nat. Genet. *53*, 435–444. https://doi.org/10.1038/s41588-021-00805-2.
52. Daniloski, Z., Jordan, T.X., Wessels, H.H., Hoagland, D.A., Kasela, S., Legut, M., Maniatis, S., Mimitou, E.P., Lu, L., Geller, E., et al. (2021). Identification of Required Host Factors for SARS-CoV-2 Infection in Human Cells. Cell *184*, 92–105.e16. https://doi.org/10.1016/j.cell.2020.10.030.
53. Zhu, Y., Feng, F., Hu, G., Wang, Y., Yu, Y., Zhu, Y., Xu, W., Cai, X., Sun, Z., Han, W., et al. (2021). A genome-wide CRISPR screen identifies host factors that regulate SARS-CoV-2 entry. Nat. Commun. *12*, 961. https://doi.org/10.1038/s41467-021-21213-4.
54. Zhou, Y.Q., Wang, K., Wang, X.Y., Cui, H.Y., Zhao, Y., Zhu, P., and Chen, Z.N. (2022). SARS-CoV-2 pseudovirus enters the host cells through spike protein-CD147 in an Arf6-dependent manner. Emerg. Microbes Infect. *11*, 1135–1144. https://doi.org/10.1080/22221751.2022.2059403.
55. Khan, N.,A.Z., Baral, A., Geiger, J.D., and Chen, X. (2022). Dimethoxycurcumin Acidifies Endolysosomes and Inhibits SARS-CoV-2 Entry. Front. Virol. *2*, 923018. https://doi.org/10.3389/fviro.2022.923018.
56. de Duve, C. (2005). The lysosome turns fifty. Nat. Cell Biol. *7*, 847–849. https://doi.org/10.1038/ncb0905-847.
57. Zhang, Y., Sun, H., Pei, R., Mao, B., Zhao, Z., Li, H., Lin, Y., and Lu, K. (2021). The SARS-CoV-2 protein ORF3a inhibits fusion of autophagosomes with lysosomes. Cell Discov. *7*, 31. https://doi.org/10.1038/s41421-021-00268-z.
58. Gobeil, L.A., Lodge, R., and Tremblay, M.J. (2013). Macropinocytosis-like HIV-1 internalization in macrophages is CCR5 dependent and leads to efficient but delayed degradation in endosomal compartments. J. Virol. *87*, 735–745. https://doi.org/10.1128/JVI.01802-12.
59. Fredericksen, B.L., Wei, B.L., Yao, J., Luo, T., and Garcia, J.V. (2002). Inhibition of endosomal/lysosomal degradation increases the infectivity of human immunodeficiency virus. J. Virol. *76*, 11440–11446.
60. Talloczy, Z., Virgin, H.W.t., and Levine, B. (2006). PKR-dependent autophagic degradation of herpes simplex virus type 1. Autophagy *2*, 24–29. https://doi.org/10.4161/auto.2176.
61. Wu, Y., Yang, X., Yao, Z., Dong, X., Zhang, D., Hu, Y., Zhang, S., Lin, J., Chen, J., An, S., et al. (2020). C19orf66 interrupts Zika virus replication by inducing lysosomal degradation of viral NS3. PLoS Negl. Trop. Dis. *14*, e0008083. https://doi.org/10.1371/journal.pntd.0008083.
62. Lin, Y., Wu, C., Wang, X., Kemper, T., Squire, A., Gunzer, M., Zhang, J., Chen, X., and Lu, M. (2019). Hepatitis B virus is degraded by autophagosome-lysosome fusion mediated by Rab7 and related components. Protein Cell *10*, 60–66. https://doi.org/10.1007/s13238-018-0555-2.
63. Ghosh, S., Dellibovi-Ragheb, T.A., Kerviel, A., Pak, E., Qiu, Q., Fisher, M., Takvorian, P.M., Bleck, C., Hsu, V.W., Fehr, A.R., et al. (2020). beta-Coronaviruses Use Lysosomes for Egress Instead of the Biosynthetic Secretory Pathway. Cell *183*, 1520–1535.e1514. https://doi.org/10.1016/j.cell.2020.10.039.
64. Bar-On, Y.M., Flamholz, A., Phillips, R., and Milo, R. (2020). SARS-CoV-2 (COVID-19) by the numbers. Elife *9*, e57309. https://doi.org/10.7554/eLife.57309.

65. Lau, S.Y., Wang, P., Mok, B.W.Y., Zhang, A.J., Chu, H., Lee, A.C.Y., Deng, S., Chen, P., Chan, K.H., Song, W., et al. (2020). Attenuated SARS-CoV-2 variants with deletions at the S1/S2 junction. Emerg. Microbes Infect. *9*, 837–842. https://doi.org/10.1080/22221751.2020.1756700.
66. Coutard, B., Valle, C., de Lamballerie, X., Canard, B., Seidah, N.G., and Decroly, E. (2020). The spike glycoprotein of the new coronavirus 2019-nCoV contains a furin-like cleavage site absent in CoV of the same clade. Antiviral Res. *176*, 104742. https://doi.org/10.1016/j.antiviral.2020.104742.
67. Brecher, M., Schornberg, K.L., Delos, S.E., Fusco, M.L., Saphire, E.O., and White, J.M. (2012). Cathepsin cleavage potentiates the Ebola virus glycoprotein to undergo a subsequent fusion-relevant conformational change. J. Virol. *86*, 364–372. https://doi.org/10.1128/JVI.05708-11.
68. Ju, X., Yan, Y., Liu, Q., Li, N., Sheng, M., Zhang, L., Li, X., Liang, Z., Huang, F., Liu, K., et al. (2015). Neuraminidase of Influenza A Virus Binds Lysosome-Associated Membrane Proteins Directly and Induces Lysosome Rupture. J. Virol. *89*, 10347–10358. https://doi.org/10.1128/JVI.01411-15.
69. Bullough, P.A., Hughson, F.M., Skehel, J.J., and Wiley, D.C. (1994). Structure of influenza haemagglutinin at the pH of membrane fusion. Nature *371*, 37–43. https://doi.org/10.1038/371037a0.
70. Staring, J., Raaben, M., and Brummelkamp, T.R. (2018). Viral escape from endosomes and host detection at a glance. J. Cell Sci. *131*, jcs216259. https://doi.org/10.1242/jcs.216259.
71. Ohkuma, S., and Poole, B. (1981). Cytoplasmic vacuolation of mouse peritoneal macrophages and the uptake into lysosomes of weakly basic substances. J. Cell Biol. *90*, 656–664.
72. Chen, X., and Geiger, J.D. (2020). Janus sword actions of chloroquine and hydroxychloroquine against COVID-19. Cell. Signal. *73*, 109706. https://doi.org/10.1016/j.cellsig.2020.109706.
73. Ooi, E.E., Chew, J.S.W., Loh, J.P., and Chua, R.C.S. (2006). In vitro inhibition of human influenza A virus replication by chloroquine. Virol. J. *3*, 39. https://doi.org/10.1186/1743-422X-3-39.
74. Di Trani, L., Savarino, A., Campitelli, L., Norelli, S., Puzelli, S., D'Ostilio, D., Vignolo, E., Donatelli, I., and Cassone, A. (2007). Different pH requirements are associated with divergent inhibitory effects of chloroquine on human and avian influenza A viruses. Virol. J. *4*, 39. https://doi.org/10.1186/1743-422X-4-39.
75. Vigerust, D.J., and McCullers, J.A. (2007). Chloroquine is effective against influenza A virus in vitro but not in vivo. Influenza Other Respir. Viruses *1*, 189–192. https://doi.org/10.1111/j.1750-2659.2007.00027.x.
76. Paton, N.I., Lee, L., Xu, Y., Ooi, E.E., Cheung, Y.B., Archuleta, S., Wong, G., and Wilder-Smith, A. (2011). Chloroquine for influenza prevention: a randomised, double-blind, placebo controlled trial. Lancet Infect. Dis. *11*, 677–683. https://doi.org/10.1016/S1473-3099(11)70065-2.
77. Tsai, W.P., Nara, P.L., Kung, H.F., and Oroszlan, S. (1990). Inhibition of human immunodeficiency virus infectivity by chloroquine. AIDS Res. Hum. Retroviruses *6*, 481–489. https://doi.org/10.1089/aid.1990.6.481.
78. Sperber, K., Louie, M., Kraus, T., Proner, J., Sapira, E., Lin, S., Stecher, V., and Mayer, L. (1995). Hydroxychloroquine treatment of patients with human immunodeficiency virus type 1. Clin. Ther. *17*, 622–636. https://doi.org/10.1016/0149-2918(95)80039-5.
79. Sperber, K., Chiang, G., Chen, H., Ross, W., Chusid, E., Gonchar, M., Chow, R., and Liriano, O. (1997). Comparison of hydroxychloroquine with zidovudine in asymptomatic patients infected with human immunodeficiency virus type 1. Clin. Ther. *19*, 913–923. https://doi.org/10.1016/s0149-2918(97)80045-8.
80. Engchanil, C., Kosalaraksa, P., Lumbiganon, P., Lulitanond, V., Pongjunyakul, P., Thuennadee, R., Tungsawad, S., and Suwanapichon, O. (2006). Therapeutic potential of chloroquine added to zidovudine plus didanosine for HIV-1 infected children. J. Med. Assoc. Thai. *89*, 1229–1236.
81. Paton, N.I., Goodall, R.L., Dunn, D.T., Franzen, S., Collaco-Moraes, Y., Gazzard, B.G., Williams, I.G., Fisher, M.J., Winston, A., Fox, J., et al. (2012). Effects of hydroxychloroquine on immune activation and disease progression among HIV-infected patients not receiving antiretroviral therapy: a randomized controlled trial. JAMA *308*, 353–361. https://doi.org/10.1001/jama.2012.6936.
82. Jacobson, J.M., Bosinger, S.E., Kang, M., Belaunzaran-Zamudio, P., Matining, R.M., Wilson, C.C., Flexner, C., Clagett, B., Plants, J., Read, S., et al. (2016). The Effect of Chloroquine on Immune Activation and Interferon Signatures Associated with HIV-1. AIDS Res. Hum. Retroviruses *32*, 636–647. https://doi.org/10.1089/AID.2015.0336.
83. Wang, M., Cao, R., Zhang, L., Yang, X., Liu, J., Xu, M., Shi, Z., Hu, Z., Zhong, W., and Xiao, G. (2020). Remdesivir and chloroquine effectively inhibit the recently emerged novel coronavirus (2019-nCoV) in vitro. Cell Res. *30*, 269–271. https://doi.org/10.1038/s41422-020-0282-0.
84. Yao, X., Ye, F., Zhang, M., Cui, C., Huang, B., Niu, P., Liu, X., Zhao, L., Dong, E., Song, C., et al. (2020). In Vitro Antiviral Activity and Projection of Optimized Dosing Design of Hydroxychloroquine for the Treatment of Severe Acute Respiratory Syndrome Coronavirus 2 (SARS-CoV-2). Clin. Infect. Dis. *71*, 732–739. https://doi.org/10.1093/cid/ciaa237.
85. Liu, J., Cao, R., Xu, M., Wang, X., Zhang, H., Hu, H., Li, Y., Hu, Z., Zhong, W., and Wang, M. (2020). Hydroxychloroquine, a less toxic derivative of chloroquine, is effective in inhibiting SARS-CoV-2 infection in vitro. Cell Discov. *6*, 16. https://doi.org/10.1038/s41421-020-0156-0.
86. Hoffmann, M., Mosbauer, K., Hofmann-Winkler, H., Kaul, A., Kleine-Weber, H., Kruger, N., Gassen, N.C., Muller, M.A., Drosten, C., and Pohlmann, S. (2020). Chloroquine does not inhibit infection of human lung cells with SARS-CoV-2. Nature *585*, 588–590. https://doi.org/10.1038/s41586-020-2575-3.
87. Mitja, O., Corbacho-Monne, M., Ubals, M., Alemany, A., Suner, C., Tebe, C., Tobias, A., Penafiel, J., Ballana, E., Perez, C.A., et al. (2021). A Cluster-Randomized Trial of Hydroxychloroquine for Prevention of Covid-19. N. Engl. J. Med. *384*, 417–427. https://doi.org/10.1056/NEJMoa2021801.
88. Abella, B.S., Jolkovsky, E.L., Biney, B.T., Uspal, J.E., Hyman, M.C., Frank, I., Hensley, S.E., Gill, S., Vogl, D.T., Maillard, I., et al. (2021). Efficacy and Safety of Hydroxychloroquine vs Placebo for Pre-exposure SARS-CoV-2 Prophylaxis Among Health Care Workers: A Randomized Clinical Trial. JAMA Intern. Med. *181*, 195–202. https://doi.org/10.1001/jamainternmed.2020.6319.
89. Sivapalan, P., Ulrik, C.S., Lapperre, T.S., Bojesen, R.D., Eklöf, J., Browatzki, A., Wilcke, J.T., Gottlieb, V., Håkansson, K.E.J., Tidemandsen, C., et al. (2022). Azithromycin and hydroxychloroquine in hospitalised patients with confirmed COVID-19: a randomised double-blinded placebo-controlled trial. Eur. Respir. J. *59*, 2100752. https://doi.org/10.1183/13993003.00752-2021.
90. Barnabas, R.V., Brown, E.R., Bershteyn, A., Stankiewicz Karita, H.C., Johnston, C., Thorpe, L.E., Kottkamp, A., Neuzil, K.M., Laufer, M.K., Deming, M., et al. (2021). Hydroxychloroquine as Postexposure Prophylaxis to Prevent Severe Acute Respiratory Syndrome Coronavirus 2 Infection : A Randomized Trial. Ann. Intern. Med. *174*, 344–352. https://doi.org/10.7326/M20-6519.
91. Arabi, Y.M., Gordon, A.C., Derde, L.P.G., Nichol, A.D., Murthy, S., Beidh, F.A., Annane, D., Swaidan, L.A., Beane, A., Beasley, R., et al. (2021). Lopinavir-ritonavir and hydroxychloroquine for critically ill patients with COVID-19: REMAP-CAP randomized controlled trial. Intensive Care Med. *47*, 867–886. https://doi.org/10.1007/s00134-021-06448-5.
92. Turk, B., Dolenc, I., Lenarcic, B., Krizaj, I., Turk, V., Bieth, J.G., and Björk, I. (1999). Acidic pH as a physiological regulator of human cathepsin L activity. Eur. J. Biochem. *259*, 926–932. https://doi.org/10.1046/j.1432-1327.1999.00145.x.
93. Nash, B., Tarn, K., Irollo, E., Luchetta, J., Festa, L., Halcrow, P., Datta, G., Geiger, J.D., and Meucci, O. (2019). Morphine-Induced Modulation of Endolysosomal Iron Mediates Upregulation of Ferritin Heavy Chain in Cortical Neurons. eNeuro *6*, ENEURO.0237-19.2019. https://doi.org/10.1523/ENEURO.0237-19.2019.

STAR★METHODS

KEY RESOURCES TABLE

REAGENT or RESOURCE	SOURCE	IDENTIFIER
Antibodies		
Biotin labeled anti-SLC38A9	Cusabio	Cat# CSB-PA836713LD01HU; RRID: N/A
Biotin labeled secondary	Thermo Fisher	Cat# A18907; RRID: AB_2535682
HRP labeled secondary (goat anti-mouse)	Thermo Fisher	Cat# A16066; RRID: AB_2534739
HRP labeled secondary (goat anti-rabbit)	Thermo Fisher	Cat# 65–6120; RRID: AB_2533967
SARS-CoV-2 S1	Sino-Biological	Cat# 40591-MM43; RRID: AB_2857934
SLC38A9	Abcam	Cat#: ab130398; RRID: AB_11159274
GAPDH	Abcam	Cat#: ab8245; RRID: AB_2107448
Chemicals, peptides, and recombinant proteins		
DMEM	Thermo Fisher	10565018
MEM	Thermo Fisher	11095098
FBS	Thermo Fisher	16140071
PBS	Thermo Fisher	10010023
Penicillin/Streptomycin	Thermo Fisher	15140122
Protein G microbeads	R&D Systems	BT10569
Cell Lysis Buffer	Thermo Fisher	1861603
SARS-CoV-2 S1 protein	Genscript	Z03501
SARS-CoV-2 S1 protein	Abcam	ab273068
Mutant SARS-CoV-2 S1 protein	Sigma	AGX818
Polybrene	Santa Cruz	sc-134220
Puromycin	Sigma-Aldrich	P4512-1MLX10
pHrodo green dextran	Thermo Fisher	P35368
Texas Red Dextran	Thermo Fisher	D1863
Hibernate E Low Fluorescence Media	Transnetyx	HELF
Intracellular pH Calibration Kit	Thermo Fisher	P35379
BODIPY FL-Pepstatin A	Thermo Fisher	P12271
LysoTracker red DND-99	Thermo Fisher	L7528
Lysotracker Green	Thermo Fisher	L7526
Protease Inhibitor Cocktail tablets	Roche	11697498001
Opti-MEM Reduced Serum media	Thermo Fisher	31985062
Lipofectamine 2000	Thermo Fisher	11668019
Critical commercial assays		
ACE2: Spike S1 RBD inhibitor screening assay	BPS Bioscience	79936
SuperSignal™ West Pico PLUS Chemiluminescent Substrate	ThermoFisher	34580
SARS-CoV-2 spike protein-conjugated pseudovirus	BPS Bioscience	79942
SARS-CoV-1 spike protein-conjugated pseudovirus	BPS Bioscience	78614
ONE-Step™ luciferase assay	BPS Bioscience	60690
Experimental models: Cell lines		
Calu-3	ATCC	HTB-55
Caco-2	ATCC	HTB-37

(*Continued on next page*)

Continued

REAGENT or RESOURCE	SOURCE	IDENTIFIER
A549	ATCC	CRM-CCL-185
U87MG	ATCC	HTB-14
Oligonucleotides		
SLC38A9 shRNA lentiviral particles (a) CCAGCTTTTGGGCCATATC (b) CCCTAGCAGTGACACCCTG (c) GTGGCTAACCTGATTGTTC	Santa Cruz	sc-91984-V
Control shRNA lentiviral particles	Santa Cruz	sc-108080
SLC38A9 siRNA (a) CUAAGAUAAUUGAAAGCGA (b) CCUGAAGGCUGUUCGUUA (c) GCUAUGAACAAGCGGAUUC (d) GGCCUAAGUUGGUGUUUCA.	Dharmacon	L-007337-02
Control siRNA	Dharmacon	D-001810-0X
Software and algorithms		
Imaris 10.1	Bitplane	https://imaris.oxinst.com/?gad_source=1&gclid=EAIaIQobChMIyMH1zLTbhgMVlDHUAR3-xg6zEAAYASAAEgK83fD_BwE
Prism 10.2.3	GraphPad	https://www.graphpad.com/features

RESOURCE AVAILABILITY

Lead contact

Further information and requests for resources and reagents should be directed to and will be fulfilled by the lead contact, Xuesong Chen (xuesong.chen@und.edu).

Materials availability

SLC38A9 knockdown U87MG cell line and SLC38A9-RFP plasmid generated in this manuscript is available from the lead contact upon request.

Data and code availability

- Datasets reported in this paper are not composed of standardized datatypes.
- No original code was reported in the paper.
- Any additional information required to reanalyze the data reported in this paper is available from the lead contact upon request.

EXPERIMENTAL MODEL AND STUDY PARTICIPANT DETAILS

Cells

Calu-3 human lung adenocarcinoma cells, Caco-2 human colorectal adenocarcinoma cells, A549 human lung adenocarcinoma cells, and U87MG human glioblastoma cells were purchased from ATCC and cultured in 1X EMEM or DMEM supplemented with 10% fetal bovine serum (FBS) and 1X penicillin and streptomycin antibiotic at 37°C in 5% CO2 incubator. For our experiments, cells were not used after 10 passages.

METHOD DETAILS

Pulldown and immunoprecipitation

For pulldown assay, protein G microbeads were preincubated with biotin-labeled SARS-CoV-2 S1 proteins (R&D, # BT10569) followed by incubation with total U87MG cell lysates (lysed in cell lysis buffer: 50 mM Tris [pH 8.0], 10 mM EDTA, 125 mM NaCl, 1% Triton X-100, proteinase inhibitor mixture) for overnight at 4°C. After washing with PBS-T, target proteins were eluted and examined with immunoblotting. For immunoprecipitation assay, protein G microbeads were preincubated with 1 μg of biotin-labeled anti-SLC38A9 (Cusabio, #Q8NBW4) with a biotin-labeled secondary antibody (ThermoFisher, # A18907) as a control followed by incubation with total U87MG cell lysates. After washing, protein G microbeads were incubated with SARS-CoV-2 S1 protein (GenScript, #Z03501) or mutant SARS-CoV-2 S1 protein lacking the multibasic (RRAR) domain (Sigma, #AGX818) overnight at 4°C. After washing with PBS-T, target proteins were eluted and examined with immunoblotting.

The spike-ACE2 binding assay

The binding of SARS-CoV-2 S1 or mutant S1 lacking multibasic motif with ACE2 was assessed using the ACE2: Spike S1 RBD (SARS-CoV-2) inhibitor screening assay kit (BPS Bioscience, #79936). Briefly, in a 96-well, nickel-coated plate, ACE2-His was added after dilution, followed by a 1-h incubation at room temperature. Following washing and blocking procedures, various concentrations of either S1 protein (Abcam, ab273068) or mutant S1 protein lacking multibasic motif (Sigma, #AGX818), along with positive controls and blanks, were added to the respective wells and allowed to incubate for 1 h. The SARS-CoV-2 Spike protein receptor binding domain (RBD)-mFc (1 μg/mL) was then introduced to the wells and allowed to incubate for an additional hour at room temperature. Following washing and blocking, secondary HRP-labeled antibodies were added and incubated for 1-h. Following washing and blocking, ELISA ECL Substrate A and B were added, and chemiluminescence was visualized using a microtiter-plate reader (Synergy H1).

siRNA knockdown

For siRNA knockdown of SLC38A9, target siRNA (50 nM, Dharmacon) and control siRNA (50 nM, Dharmacon) were dissolved in Accell1 transfection media (B-005000, Dharmacon) and DharmaFECT 1 (T-2001-02, Dharmacon) was used as transfection reagent for U87MG cells. The Dharmacon ON-TARGET plus Human SLC38A9 siRNA SMART pool comprising of 4 siRNA sequences targeting the ORF was used with the sequences as follows: (a) CUAAGAUAAUUGAAAGCGA, (b) CCUGAAGGCUGUUCGUUA (c) GCUAUGAACAAGCGGAUUC (d) GGCCUAAGUUGGU GUUUCA. The ON-TARGETplus Non-targeting Control siRNA was used as control. Knockdown efficiency for SLC38A9 was determined with immunoblotting.

Generating SLC38A9 knockdown stable cell line

SLC38A9 knockdown U87MG cell lines were established using stable expression of short hairpin RNAs (shRNAs) that target SLC38A9 mRNA. Cells were transduced with SLC38A9 shRNA lentiviral particles (sc-91984-V, Santa Cruz) or control shRNA lentiviral particles (sc-108080, Santa Cruz). The SLC38A9 Lentiviral shRNA (sc-91984-v) sequences comprise three expression constructs with the sequences as follows: (a) CCAGCTTTTGGGCCATATC (b) CCCTAGCAGTGACACCCTG (c) GTGGCTAACCTGATTGTTC. Transductions of cells were carried out in the presence of 8 μg/mL of polybrene (sc-134220, Santa Cruz). After mixing with polybrene, the viral stocks were added to the cells (1 × 104 cells/well in 96 well plates) at the multiplicity of infection (MOI) of 10. After 24 h of transduction, the cells were collected, and then fresh media lacking polybrene were added to them. The transduced cells were allowed to proliferate until a sufficient cell number was reached for puromycin selection, which was performed to select stable clones expressing the shRNA. The cell culture medium was replaced with a fresh medium plus 1 μg/mL of puromycin (optimal concentration of selection) every 2 to 3 days until resistant clones appeared. After 3–4 weeks, the cells were collected and examined for SLC38A9 expression using immunoblotting. The selected clones were maintained in the fresh puromycin-containing medium for an additional month, analyzed, and used for further experiments.

Endolysosome pH measurement

Total endolysosome pH was measured using a combination of dextran labeling as done previously.[93] Briefly, cells were plated on 35 mm glass bottom Poly-D-lysine dishes, and after 24 h loaded with10 μg/mL each of pH sensitive pHrodo Green Dextran (P35368, ThermoFisher) and pH insensitive dextran, Texas Red (D1863, ThermoFisher) for another 24 h. The following morning, dextran containing medium was washed off twice with PBS, and cells transferred to Hibernate E Low Fluorescence Medium (HELF, Brainbits) at 37°C for imaging. SARS-CoV-2 S1 (GenScript, #Z03501), or mutant SARS-CoV-2 S1 protein lacking multibasic motif (Sigma, #AGX818) was added at mentioned concentrations and fluorescence emission at 533 nm and 615 nm measured for Green and Texas Red dextran respectively. The ratio of 615/533 was converted to pH using an intracellular pH calibration kit (P35379, ThermoFisher) with the addition of 10 μM nigericin and 20 μM Monensin in Hibernate E Flow Fluorescence (HELF) Media adjusted to different pH with HCl or NaOH. For all pH imaging and measurements, a total of 5 fields under 40× on a Zeiss LSM800 confocal microscope comprising of at least 5–10 cells/field were imaged, and three independent experiments were carried out.

Active cathepsin D staining

Active cathepsin D was identified in cells stained with BODIPY-FL Pepstatin A (P12271, ThermoFisher) and total endolysosomes were identified with LysoTracker red DND-99. Briefly, cells were incubated with LysoTracker (10 nM) and with BODIPY-FL Pepstatin A (1 μM) for 30 min at 37°C. Following washing, fresh warm Hibernate E low fluorescence (HELF) media were added for imaging under the 63× objective of a Zeiss LSM 800 confocal microscope using 0.5 μm z stack intervals. 25–30 cells by per treatment group were imaged and experiments were repeated independently three times. Total endolysosomes (LysoTracker) and active cathepsin D positive endolysosomes (BODIPY-FL Pepstatin A) were reconstructed as spots using Imaris 10.1 software. Percentage of active cathepsin D-positive endolysosomes vs. total endolysosomes was calculated.

Cellular entry of SARS-CoV-2 spike protein pseudo-virus

The SARS-CoV-2 Spike Pseudotyped Lentivirus were produced with SARS-CoV-2 Spike (GenBank Accession #QHD43416.1) as the envelope glycoproteins. These pseudovirions also contain the firefly luciferase gene driven by a CMV promoter (BPS Biosciences, #79942), therefore, the spike-mediated cell entry can be measured via luciferase reporter activity in a Biosafety Level 2 facility. Briefly, cells cultured on 96-well

plates were treated with luciferase-integrated and SARS-CoV-2 spike protein-conjugated pseudovirus for 6 h, washed 3-times with media and incubated for another 36 h according to the manufacturer protocol (BPS Biosciences, #79942). Post-incubation, S protein-mediated entry of SARS-CoV-2 pseudovirus was estimated by luciferase activity, which was determined with a ONE-Step luciferase assay system (BPS Bioscience #60690). Luciferase activity was measured as luminescence relative light unit (RLU) using microplate reader (Synergy H1).

Cellular entry of SARS-CoV-1 spike protein pseudo-virus

The Spike (SARS-CoV-1) Pseudotyped Lentiviruses were produced with SARS-CoV-1 Spike (GenBank Accession #YP_009825051.1) as the envelope glycoprotein. These pseudovirions also contain the firefly luciferase gene driven by a CMV promoter (BPS Biosciences, #78614), therefore, the spike-mediated cell entry can be measured via luciferase reporter activity. Briefly, cells (10k per well) cultured on 96-well plates were treated with luciferase-integrated and SARS-CoV-1 spike protein-conjugated pseudovirus (5 μL) for 48 h according to the manufacturer protocol (BPS Biosciences, #78614). Post-incubation, S protein-mediated entry of SARS-CoV-2 pseudovirus was estimated by luciferase activity, which was determined with a ONE-Step luciferase assay system (BPS Bioscience #60690). Luciferase activity was measured as luminescence relative light unit (RLU) using microplate reader (Synergy H1).

SLC38A9-RFP expression

SLC38A9-RFP cloned into pCMV6-AC-RFP vector was obtained from Origene Technologies (Rockville, MD). Lipofectamine 2000 transfection Reagent (11668019, ThermoFisher) was used for transient transfections, cells plated on either 35 mm glass bottom dishes or 18 mm coverslips were transfected with 1–2 μg of plasmid DNA/well in Opti-MEM Reduced Serum media (31985062, ThermoFisher) for 48 h.

Live cell imaging

U87MG cells or SLC38A9-RFP expressing U87MG cells were treated with Alexa 488 labeled SARS-CoV-2 S1 (AFG10878–020, R&Dsystem) for 1 h and/or LysoTracker Green (10 nM) for 15 min at 37°C. Live cell images were acquired under the 63× objective of a Zeiss LSM 800 confocal microscope using 0.5 μm z stack intervals. Co-localization was analyzed Imaris 10.1 (Bitplane).

Immunoblotting

SDS-PAGE (4–12% gel) was used to separate total cell lysate proteins (10 μg/lane) and blots were transferred to nitrocellulose membranes using the iBlot 2 dry transfer system (Invitrogen). Membranes were incubated overnight at 4°C with antibodies against SARS-CoV-2 S1 (SinoBiological, #40591-MM43), SLC38A9 (Abcam, ab130398), actin (Abcam, ab8226), GAPDH (Abcam, ab8245). Blots were developed with enhanced chemiluminescence, and the density of antibody-positive protein bands was determined using an Odyssey Fc Imaging System (LiCor).

QUANTIFICATION AND STATISTICAL ANALYSIS

Statistical analyses were performed using GraphPad software (version 10.2.3). All data were presented as mean ± SEM. The number of independent repeats was used to calculate n. Statistical significance between two groups was determined with Student's t test, and statistical significance among multiple groups was determined using a one-way or two-way ANOVA. $p < 0.05$ was accepted to be statistically significant.